Supporting Information for

Efficacious Elimination of Intramolecular Charge Transfer in Perylene Imide Based Light-Harvesting Antenna Molecules

Rajeev K. Dubey,[#] Damla Inan, Abbey M. Philip, Ferdinand C. Grozema and Wolter F. Jager**

Department of Chemical Engineering, Delft University of Technology, Van der Maasweg 9, 2629 HZ Delft, The Netherlands.

Table of Contents

1. Experimental Details

1.1 Materials: The compounds 1,7-dibromoperylene monoanhydride diester (**1**), 1,6,7,12-tetrachloroperylene bisanhydride (**4**), **A2**, and **A4** were synthesized according to the previously described procedures.[1,2,3] All other reagents utilized in the syntheses were used as received from the manufacturers, unless otherwise stated. The NMP used in the synthesis was of anhydrous grade. Toluene was dried over sodium under an argon atmosphere prior to use.

1.2 Instrumentation and Characterization: The NMR spectra were recorded with 400 MHz pulsed Fourier transform NMR spectrometer in either $CDCl_3$ or DMSO-d_6 at room temperature. The chemical shift values are given in ppm and *J* values in Hz. High-resolution mass spectra were collected on an AccuTOF GCv 4G, JMS-T100GCV, Mass spectrometer (JEOL, Japan). The FD/FI probe (FD/FI) was equipped with an FD Emitter, Carbotec (Germany), FD 10 µm. Typical measurement conditions were as follow: Current rate 51.2 mA/min over 1.2 min; Counter electrode –10 kV; Ion source 37 V. The samples were prepared in dichloromethane.

Absorption measurements were performed in PerkinElmer Lambda 40 UV– vis spectrophotometer. Photoluminescence studies were done in SPEX Fluorimeter. Fluorescence lifetimes were performed with LifeSpec-ps Fluorescence spectrometer with fixed excitation wavelength of 400 nm. For quantum yield measurements, the formula for optically dilute solutions was used.[4] Fluorescence quantum yields were determined by the comparative method using perylene-3,4,9,10-tetracarboxylic tetrabutylester (φ_F = 0.95 in CH_2Cl_2) and N,N´-bis(1-hexylheptyl)-perylene-3,4,9,10-tetracarboxy bisimide (φ_F = 0.99 in $CHCl_3$) as reference compounds.[5]

Pump-probe transient-absorption measurements were performed by using tunable Yb:KGW laser system consisting of a YB:KGW laser (1028 nm), which operates at 5 kHz with a pulse duration of less than 180 fs (PHAROS-SP-06-200 Light Conversion) and an optical parametric amplifier (ORPHEUS- PO15F5HNP1, Light Conversion). A white light continuum probe pulse was generated by focusing part of the fundamental 1028 nm from Pharos into a sapphire crystal. Transient absorption data were collected using a commercial pump-probe spectrometer, HELIOS (Ultrafast Systems) in the wavelength range of 490– 910 nm. The maximum time-delay between the pump and the probe pulse was 3.3 ns. The compounds were dissolved in spectroscopic grade solvents and placed in quartz cuvettes that had 2 mm path length. To prevent aggregation and photobleaching, the samples were stirred during the measurements with a magnetic stirrer. The data was taken at the magic angle (54.7˚) to prevent any polarization dependence. Transient absorption data was analyzed with global and target analysis using the open source software Glotaran.[6,7]

In order to gain insights into the nature of the excited states of the multichromophoric systems studied in this work we have performed electronic structure calculations for two representative systems **Im-D2A4** and **D2A3**. To reduce the conformational freedom in the geometry optimizations, the alkyl (butyl and tertiary butyl) chains in the structures were replaced by methyl groups, forming truncated **Im-D2A4** and **D2A3**, but otherwise the full structure was considered. The geometries were fully optimized using DFTB together with the QUASINANO parameter set in the Amsterdam Density Functional (ADF) program suite.[8] Subsequently, the lowest 30 excited states were calculated using a Singles configuration interaction approach (CIS) starting from an INDO/S ground state wave-function in the program package Gaussian09.[9] The resulting orbitals were plotted with the Avogadro software package.[10]

2. Synthesis

2.1 Synthesis of antenna system Im-D2A2:

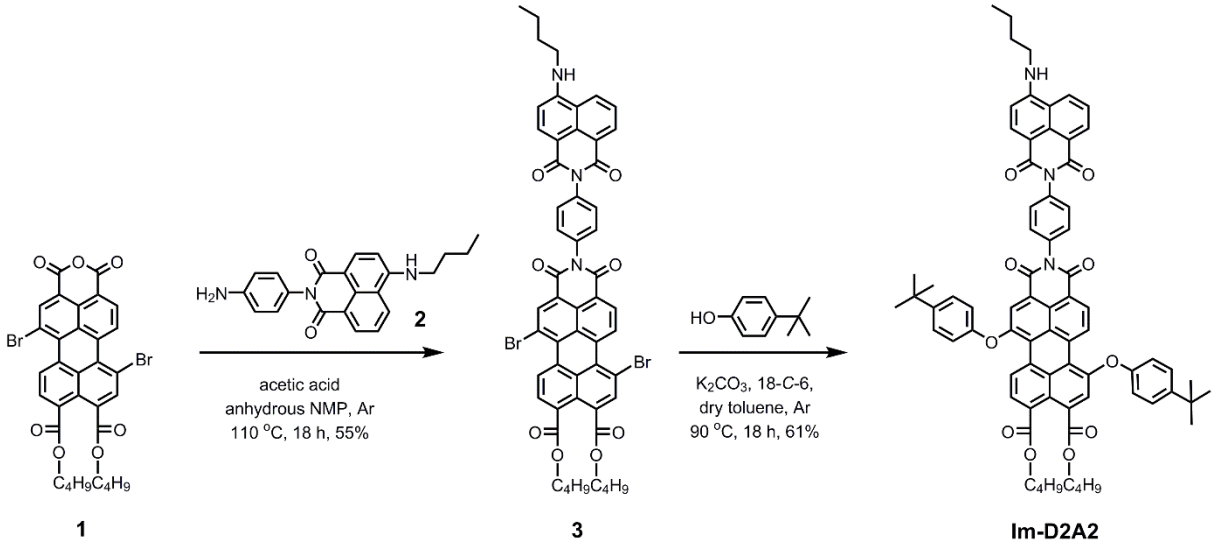

Scheme S1. Synthesis of perylene monoimide based antenna system **Im-D2A2**.

Synthesis of compound 3: A 50 mL round-bottom flask was charged with regioisomerically pure 1,7-dibromoperylene monoanhydride diester **1** (0.10 g, 0.15 mmol), compound **2** (0.16 g, 0.45 mmol), acetic acid (0.09 mL, 1.48 mmol), and anhydrous NMP (20 mL). The reaction mixture was stirred at 110 °C for 18 h under Ar atmosphere. After being cooled to room temperature, toluene (100 mL) was added to the reaction mixture and the resultant solution was washed with slightly acidic water (3 x 200 mL). Organic layer was collected and evaporated by rotary evaporation. The solid residue was chromatographed on silica (DCM to chloroform) to afford the desired product **3** (0.83 g, 55%). ^{1}H NMR (400 MHz, $CDCl_3$): δ = 9.27 (d, J = 8.0 Hz, 1H), 9.24 (d, J = 8.0 Hz, 1H), 8.93 (s, 1H), 8.72 (d, J = 8.0 Hz, 1H), 8.65 (d, J = 7.2 Hz, 1H), 8.52 (d, J = 8.0 Hz, 1H), 8.34 (s, 1H), 8.16 (t, J = 8.4 Hz, 2H), 7.66 (t, J = 8.0 Hz, 1H), 7.54–7.46 (m, 4H), 6.76 (d, J = 8.4 Hz, 1H), 4.39–4.30 (m, 4H), 3.47–3.40 (m, 2H), 1.88–1.72 (m, 6H), 1.56−1.42 (m, 6H), 1.07–0.95 ppm (m, 9H).

Synthesis of compound Im-D2A2: A mixture of 4-*tert*-butylphenol (44 mg, 0.29 mmol), anhydrous potassium carbonate (80 mg, 0.58 mmol), 18-crown-6 (160 mg, 0.60 mmol) in anhydrous toluene (100 mL) was stirred for 20 minutes at room temperature under argon atmosphere. Subsequently, compound **3** (100 mg, 0.10 mmol) was added. The reaction was continued for 18 h at 90 °C and then allowed to cool down to room temperature. The reaction mixture was extracted with water (3 x 100 mL). The organic phase was collected, and toluene was evaporated. The solid residue was chromatographed on silica, eluting with chloroform, to afford the desired product **Im-D2A2** (69 mg, 61%). ^{1}H NMR (400 MHz, $CDCl_3$): δ = 9.41 (d, J = 8.0 Hz, 1H), 9.39 (d, J = 8.0 Hz, 1H), 8.62 (d, J = 7.2

Hz, 1H), 8.60 (d, *J* = 8.4 Hz, 1H), 8.50 (d, *J* = 8.4 Hz, 1H), 8.38 (s, 1H), 8.11 (d, *J* = 8.4 Hz, 1H), 8.04 (d, *J* = 8.0 Hz, 1H), 7.77 (s, 1H), 7.62 (t, *J* = 8.0 Hz, 1H), 7.48–7.40 (m, 8H), 7.08 (d, *J* = 8.8 Hz, 2H), 7.05 (d, *J* = 8.8 Hz, 2H), 6.74 (d, *J* = 8.4 Hz, 1H), 5.29 (s, 1H), 4.30 (t, *J* = 6.4 Hz, 2H), 4.24 (t, *J* = 6.4 Hz, 2H), 3.45–3.37 (m, 2H), 1.84–1.72 (m, 4H), 1.70–1.56 (m, 4H), 1.54−1.42 (m, 4H), 1.35 (s, 9H), 1.33 (s, 9H), 1.03 (t, *J* = 7.6 Hz, 3H), 0.97 (t, *J* = 7.6 Hz, 3H), 0.89 ppm (t, *J* = 7.2 Hz, 3H). MS (ESI-TOF): $[M]^+$ Calculated for $C_{74}H_{70}N_3O_{10}$, 1160.49673; found, 1160.49972.

2.2 Synthesis of antenna system Im-D2A4:

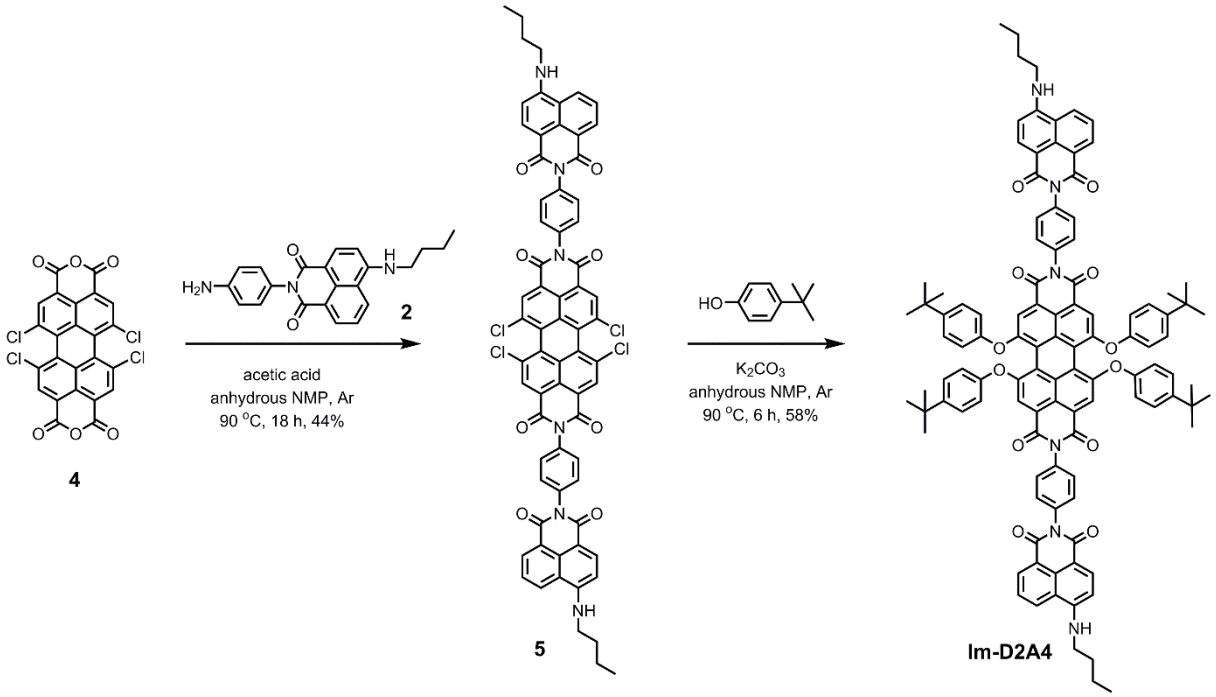

Scheme S2. Synthesis of perylene bisimide based antenna system **Im-D2A4**.

Synthesis of compound 5: A 50 mL round-bottom flask was charged with 1,6,7,12-tetrachloroperylene bisanhydride **4** (130 mg, 0.25 mmol), compound **2** (330 mg, 0.92 mmol), acetic acid (0.40 mL), and anhydrous NMP (14 mL). The reaction mixture was stirred at 90 °C for 18 h under Ar atmosphere. After being cooled to room temperature, toluene (100 mL) was added to the reaction mixture and the resultant solution was washed with slightly acidic water (3 x 200 mL). Organic layer was collected and evaporated by rotary evaporation. The solid residue was chromatographed on silica using chloroform as eluent to afford the desired product **5** (131 mg, 44%). ^{1}H NMR (400 MHz, $CDCl_3$): δ = 8.82–8.76 (m, 6H), 8.65 (d, *J* = 8.4 Hz, 2H), 8.35 (d, *J* = 8.4 Hz, 2H), 7.87 (t, *J* = 8.0 Hz, 2H), 7.58–7.50 (m, 8H), 7.20 (d, *J* = 8.4 Hz, 2H), 3.58 (t, *J* = 7.6 Hz, 4H), 1.90–1.82 (m, 4H), 1.58−1.50 (m, 4H), 1.03 ppm (t, *J* = 7.2 Hz, 6H).

Synthesis of antenna system Im-D2A4: A mixture of compound **5** (60 mg, 0.05 mmol), 4-*tert*-butylphenol (52 mg, 0.35 mmol) and anhydrous potassium carbonate (48 mg, 0.35 mmol) was stirred

for 6 h at 90 °C in anhydrous NMP (12 mL) under an inert atmosphere. After being cooled to room temperature, toluene (100 mL) was added and the reaction mixture was extracted with slightly acidic water (3 x 200 mL). The organic phase was collected, and toluene was evaporated. The solid residue was chromatographed on silica, eluting with chloroform, to afford the desired product **Im-D2A4** (48 mg, 58%). ^{1}H NMR (400 MHz, $CDCl_3$): δ = 8.61 (d, J = 7.6 Hz, 2H), 8.50 (d, J = 7.6 Hz, 2H), 8.28 (s, 4H), 8.10 (d, J = 8.4 Hz, 2H), 7.64 (t, J = 7.2 Hz, 2H), 7.46–7.40 (m, 8H), 7.23 (d, J = 7.6 Hz, 8H), 6.84 (d, J = 7.6 Hz, 8H), 6.75 (d, J = 8.4 Hz, 2H), 5.25 (s, 2H), 3.45–3.37 (m, 4H), 1.84–1.76 (m, 4H), 1.27 (s, 36H), 1.03 ppm (t, J = 7.2 Hz, 6H). MS (ESI-TOF): $[M]^+$ Calculated for $C_{108}H_{94}N_6O_{12}$, 1666.67637; found, 1666.68261.

2.3 Synthesis of naphthalene monoimide precursor 2:

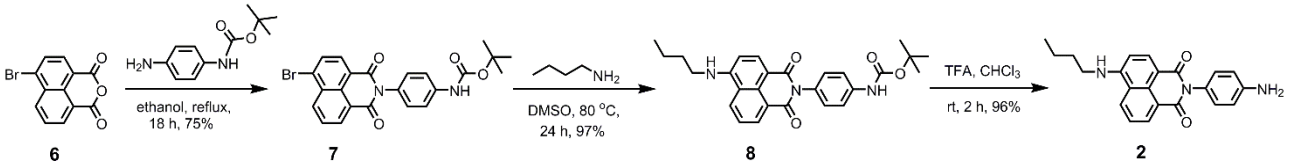

Scheme S3. Synthesis of 4-butylamino substituted naphthalene monoimide precursor **2**.

Synthesis of *N*-[(4′-Boc-amino)phenyl]-4-bromonaphthalene-1,8-dicarboxy Monoimide (7): A mixture of 4-bromo-1,8-naphthalic anhydride **6** (1.00 g, 3.61 mmol) and 4-(*N*-Boc-amino)aniline (0.90 g, 4.33 mmol), in ethanol (60 mL), was refluxed for 18 h. The reaction mixture was cooled to room temperature and the precipitate was collected by filtration. Thereafter, the precipitate was washed with ethanol and dried to obtain the compound **7** (1.27 g, 75%) as a white solid. ^{1}H NMR (400 MHz, DMSO-d6): δ = 9.49 (s, 1H), 8.61–8.55 (m, 2H), 8.33 (d, J = 8.0 Hz, 1H), 8.24 (d, J = 8.0 Hz, 1H), 8.02 (t, J = 8.0 Hz, 1H), 7.54 (d, J = 8.0 Hz, 2H), 7.22 (d, J = 8.0 Hz, 2H), 1.48 ppm (s, 9H).

Synthesis of *N*-[(4′-Boc-amino)phenyl]-4-(*n*-butylamino)naphthalene-1,8-dicarboxy Monoimide (8): A 50 mL round-bottomed flask was charged with compound **7** (0.80 g, 1.71 mmol), *n*-butylamine (2.6 mL, 1.90 g, 25.68 mmol), and DMSO (24 mL). The reaction mixture was stirred at 80 °C for 24 h and the resultant solution was poured in water (500 mL) to precipitate the crude product. The precipitate was filtered off and washed with several portions of water. Afterwards, washed with a small amount of methanol and dried in vacuum oven to afford the compound **8** (0.76 g, 97%) as yellow solid. ^{1}H NMR (400 MHz, $CDCl_3$): δ = 8.59 (d, J = 7.2 Hz, 1H), 8.48 (d, J = 8.4 Hz, 1H), 8.10 (d, J = 8.4 Hz, 1H), 7.62 (t, J = 8.0 Hz, 1H), 7.49 (d, J = 7.6 Hz, 2H), 7.20 (d, J = 7.6 Hz, 2H), 6.73 (d, J = 8.4 Hz, 1H), 6.58 (s, 1H), 5.28 (s, 1H), 3.45–3.36 (m, 2H), 1.84–1.74 (m, 2H), 1.55–1.45 (m, 11H), 1.02 ppm (t, J = 7.2 Hz, 3H).

Synthesis of *N*-(4'-aminophenyl)-4-(*n*-butylamino)naphthalene-1,8-dicarboxy Monoimide (2): Compound **8** (1.21 g, 2.63 mmol) was stirred for 2 h in a mixture of chloroform (45 mL) and CF_3COOH (10 mL) at room temperature. Afterwards, the solvents were evaporated under vacuum. The resultant residue was stirred in an aqueous solution of K_2CO_3 (pH = 9) and then filtered, washed with water, and dried to afford the compound **2** (0.91 g, 96%). ^{1}H NMR (400 MHz, DMSO-d6): δ = 8.70 (d, J = 8.4 Hz, 1H), 8.38 (d, J = 7.2 Hz, 1H), 8.21 (d, J = 8.8 Hz, 1H), 7.72 (s, 1H), 7.66 (t, J = 8.0 Hz, 1H), 6.88 (d, J = 8.4 Hz, 2H), 6.76 (d, J = 8.8 Hz, 1H), 6.66 (d, J = 8.4 Hz, 2H), 3.45–3.36 (m, 2H), 1.73–1.62 (m, 2H), 1.45–1.36 (m, 2H), 0.93 ppm (t, J = 7.2 Hz, 3H).

2.4 Attempted Syntheses of antenna system Im-D2A3:

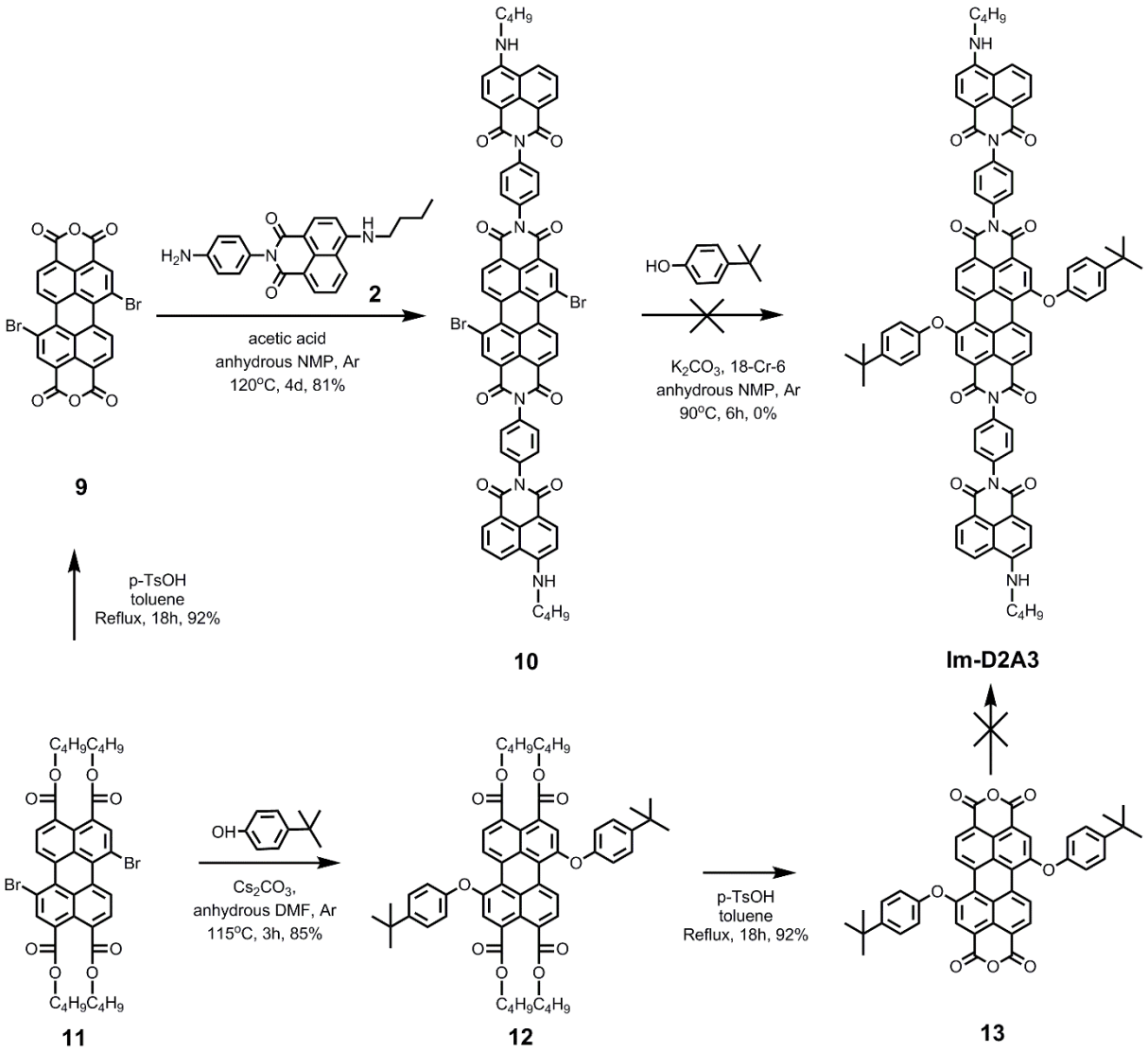

Scheme S4. Attempted syntheses of antenna system **Im-D2A3.**

Compounds **9** and **11–13** are known compounds. Compound **10** is insoluble in common organic solvents and, hence, its identity could not be confirmed.

3. Spectral data

3.1 Structure of Model Compounds:

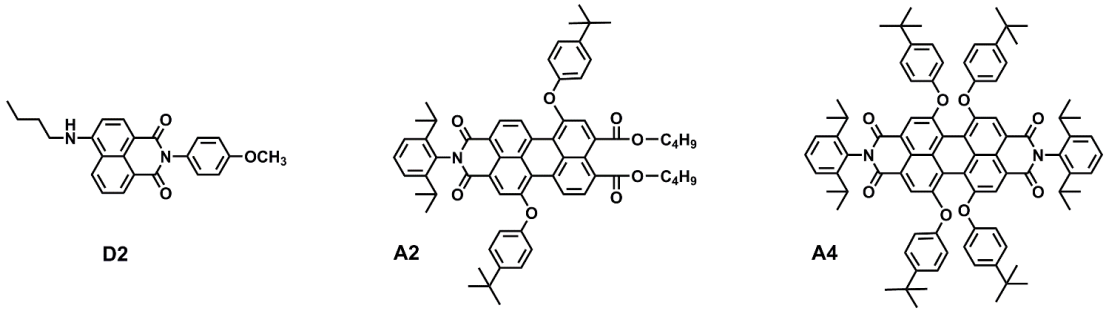

Figure S1. Model compounds **D2**, **A2** and **A4**.

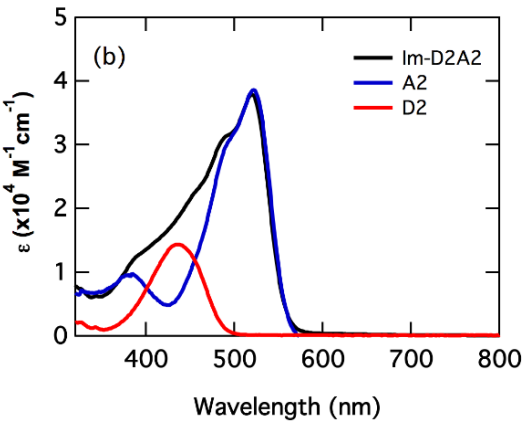

Figure S2. UV/Vis absorption spectra of antenna system **Im-D2A2** along with reference acceptor **A4** and reference donor **D2** in benzonitrile.

3.2 UV-Vis Absorption Spectra:

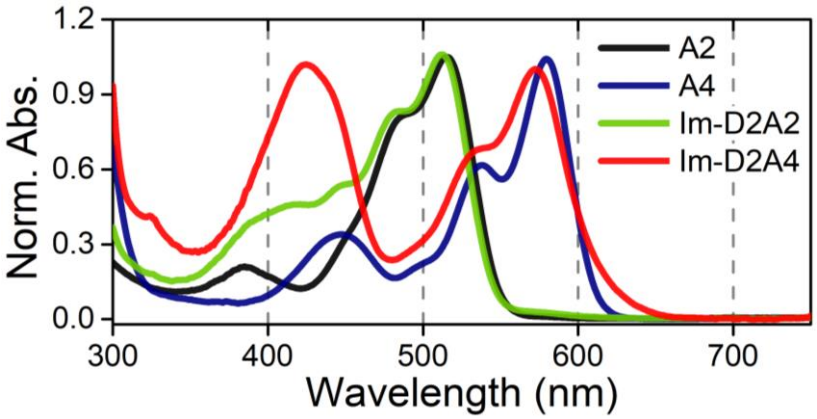

Figure S3. UV-Vis absorption spectra of **A2**, **A4**, **Im-D2A2** and **Im-D2A4** in toluene.

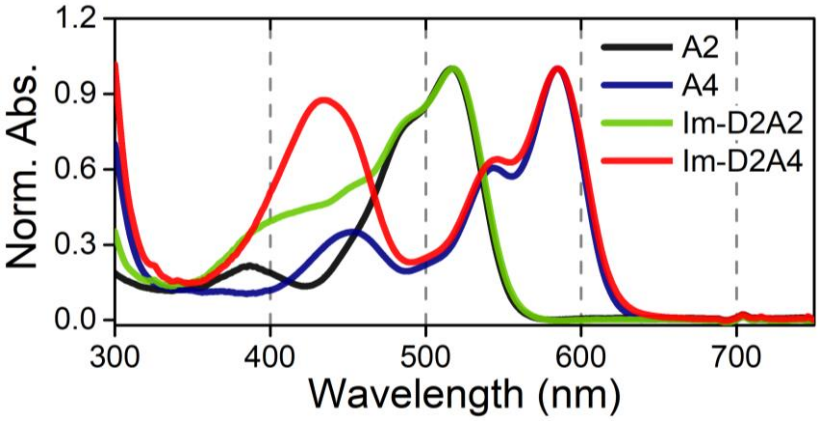

Figure S4. UV-Vis absorption spectra of **A2**, **A4**, **Im-D2A2** and **Im-D2A4** in chloroform.

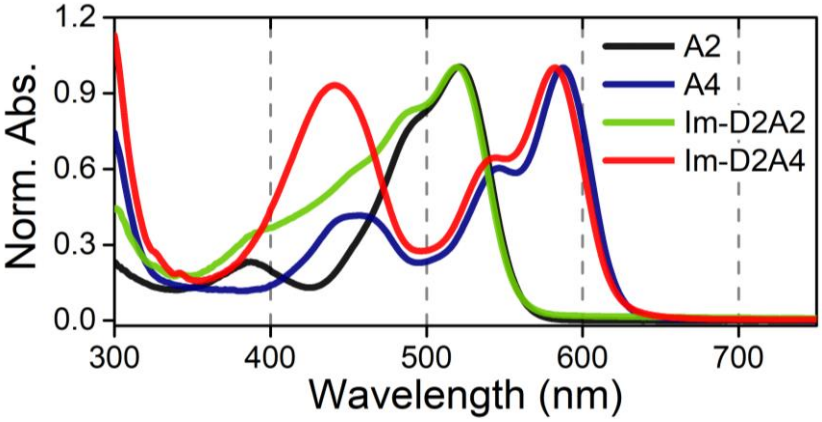

Figure S5. UV-Vis absorption spectra of **A2**, **A4**, **Im-D2A2** and **Im-D2A4** in benzonitrile.

3.3 Fluorescence Spectra:

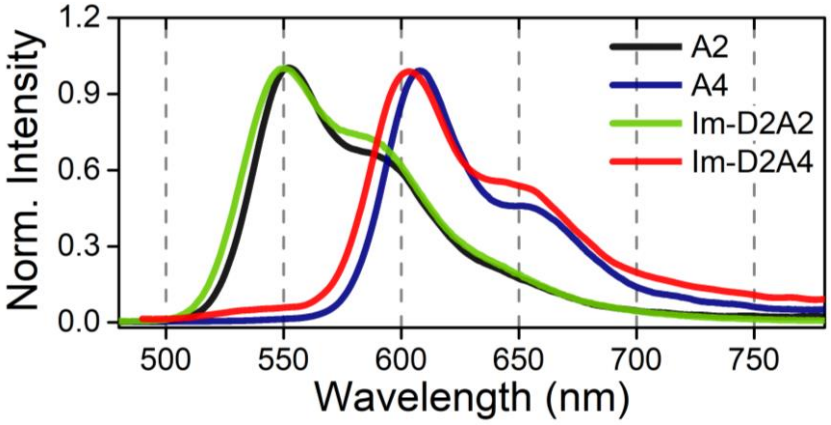

Figure S6. Fluorescence emission spectra of **A2**, **A4**, **Im-D2A2** and **Im-D2A4** in toluene.

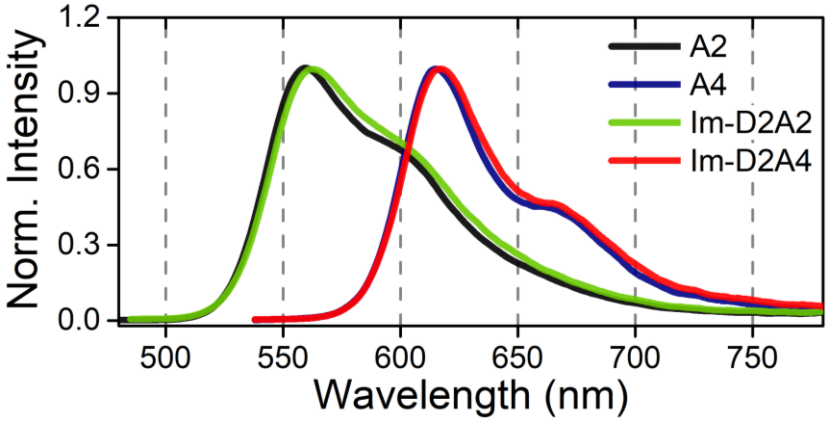

Figure S7. Fluorescence emission spectra of **A2**, **A4**, **Im-D2A2** and **Im-D2A4** in chloroform.

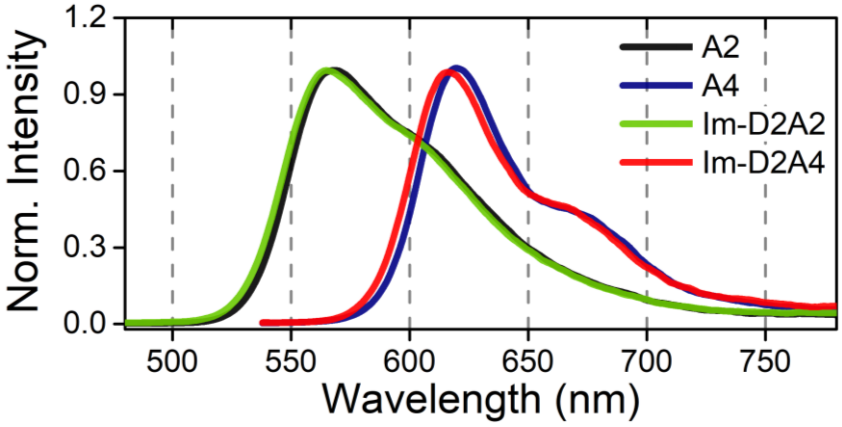

Figure S8. Fluorescence emission spectra of **A2**, **A4**, **Im-D2A2** and **Im-D2A4** in benzonitrile.

3.4 Excitation Spectrum of Im-D2A2

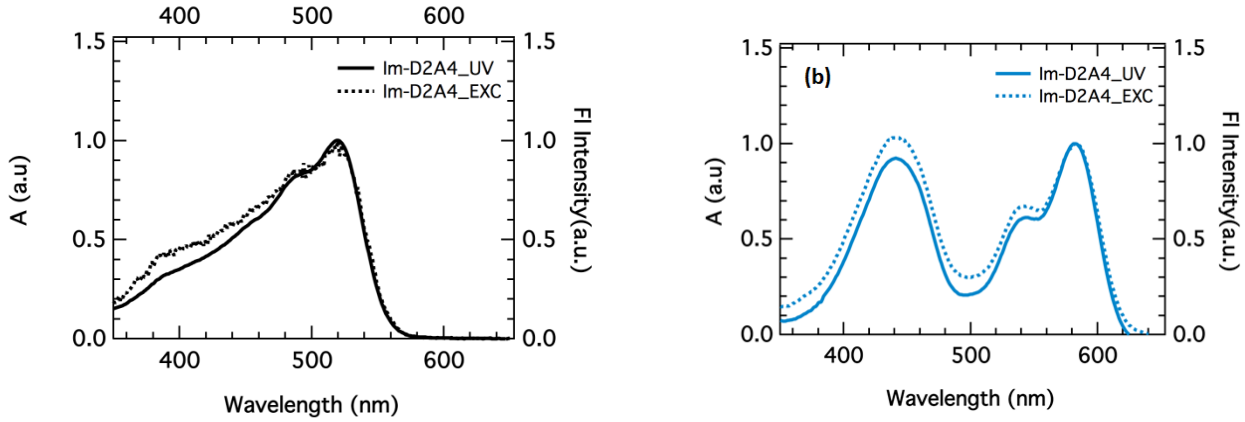

Figure S9. Comparison of absorption (solid-line) and excitation (dashed-line) spectra of **Im-D2A2** (left) and of **Im-D2A4** (right) measured at $\boldsymbol{\lambda_{em}}$ **=** 650 nm in benzonitrile.

3.5 Time Resolved Fluorescence Spectra

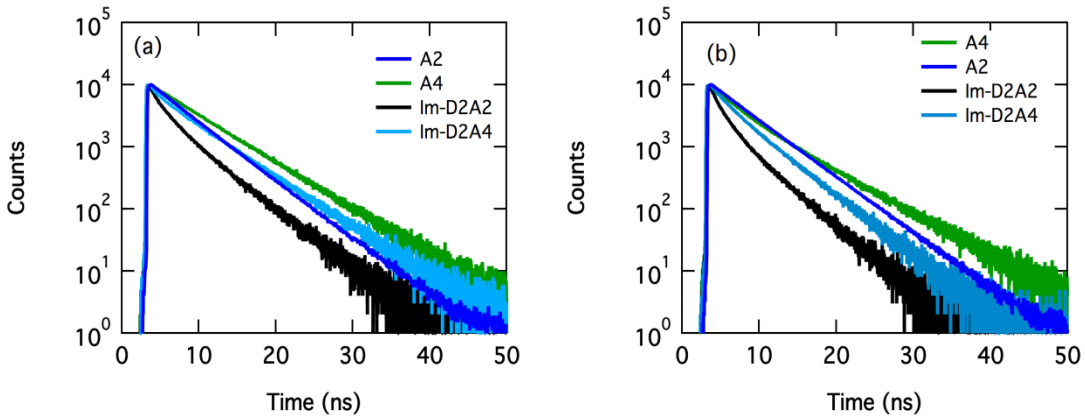

Figure S10. Time resolved fluorescence spectra of **Im-D2A2**, **Im-D2A4** and reference acceptors **A2**, **A4:** (a) in toluene (b) in benzonitrile

3.6 Rates of Fluoresence and Fluorescence Quenching

$$k_F = \frac{\phi_F}{\tau_F} \quad (Eq\ S1a) \qquad\qquad k_{nr} = \frac{k_F}{\phi_F} - k_F \quad (Eq\ S1b)$$

3.7 Förster Energy Transfer[11]

$$k_{EET} = \frac{9\kappa^2 c^4}{8\pi\tau_D n^4 r_{DA}{}^6} J(\omega) \quad \text{with} \quad J(\omega) = \int F_D(\omega)\sigma_A(\omega)\frac{d\omega}{\omega} \quad \text{(Eq S2)}$$

The rate of excitation energy transfer by EET by Förster resonance energy transfer (FRET) is given by the Förster Equation; where κ^2 is a factor describing the relative orientation of the transition dipoles

of donor and acceptor moieties, c is the speed of light, η is the refractive index, τ_D is the fluorescence lifetime of the donor, ω is an optical frequency in radians per second and $J(\omega)$ is the overlap integral that expresses the spectral overlap in donor emission and acceptor absorption. Within $J(\omega)$, $F_D(\omega)$ is the normalized florescence spectrum of the donor, $\sigma_A(\omega)$ is the linear absorption cross-section of the acceptor.

3.8 Photophysical Properties in Toluene and Chloroform

Table S1. Photo-physical properties of the reference compounds and donor-acceptor systems in toluene.

[a] Fluorescence Quantum Yield [b] Fluoresence lifetime (λ_{exc} = 400 nm) [c] limited solubility

Compound	Solvent	ϕ_F[a]	τ_F (ns)[b]
A2	toluene chloroform benzonitrile	0.92 0.88 0.82	4.52 4.80 4.55
A4	toluene chloroform benzonitrile	0.96 0.92 0.93	5.51 5.98 5.69
Im-D2A2	toluene chloroform benzonitrile	0.80 0.74 0.70	4.20 (0.81), 1.35 (0.09) 4.62 (0.93), 1.35 (0.07) 4.23 (0.90), 1.47 (0.10)
Im-D2A4	toluene chloroform benzonitrile	0.55[c] 0.81 0.61	5.34 (0.89), 1.50 (0.11) 5.47 (0.81), 1.55 (0.09) 4.45 (0.78), 1.79 (0.22)

3.9 Transient Absorption Spectra of Im-D2A4

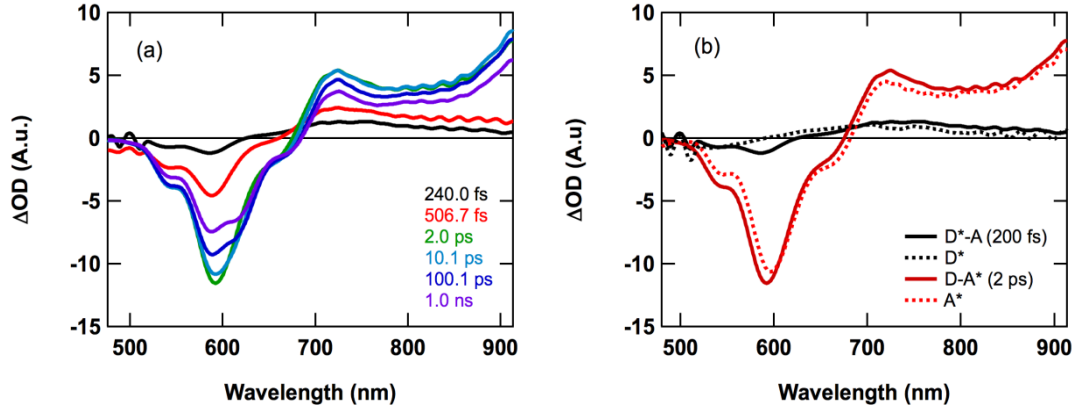

Figure S11. (a)Time evolution of the femtosecond transient absorption spectra of **Im-D2A4** excitation at 430 nm in benzonitrile (b) The spectra of **Im-D2A4** with the dissociation of species after different time delays along with reference donor and reference acceptor.

3.10 Transient Absorption Spectra of Reference Compounds

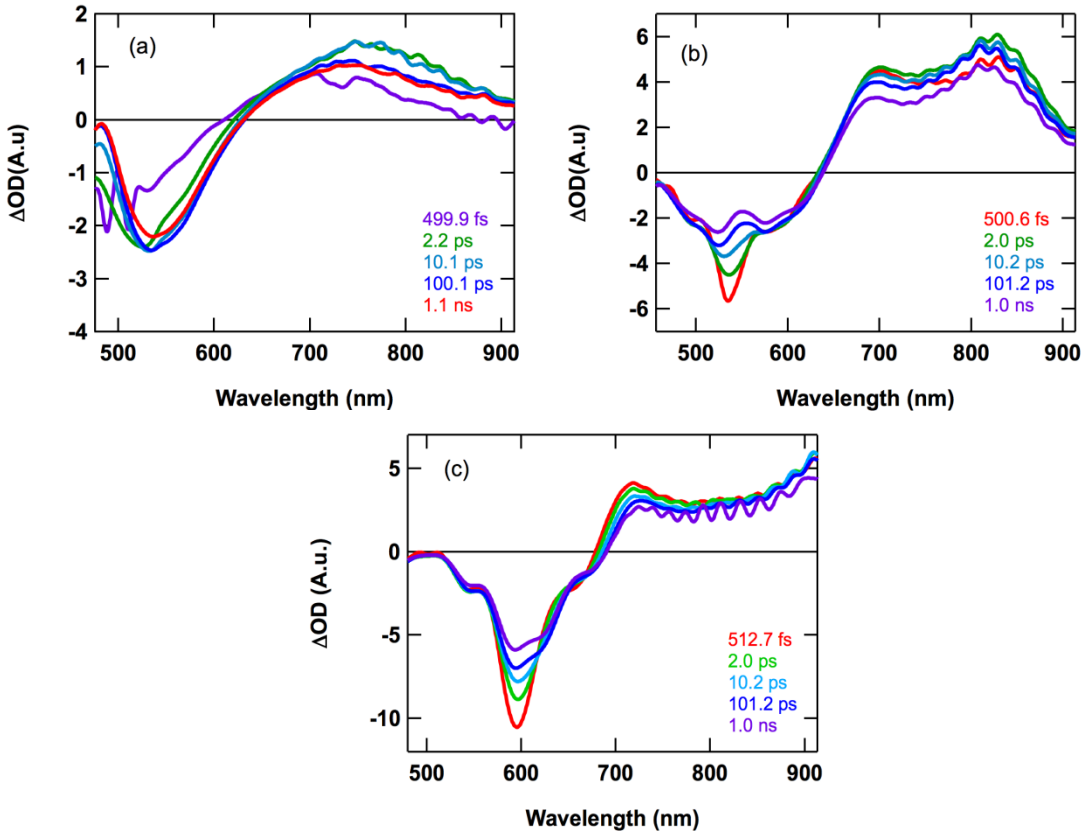

Figure S12. Time evolution of the femtosecond transient absorption spectra in benzonitrile: (a) **D2** after excitation at 430 nm (b) **A2** after excitation at 530 nm (c) **A4** after excitation at 580 nm.

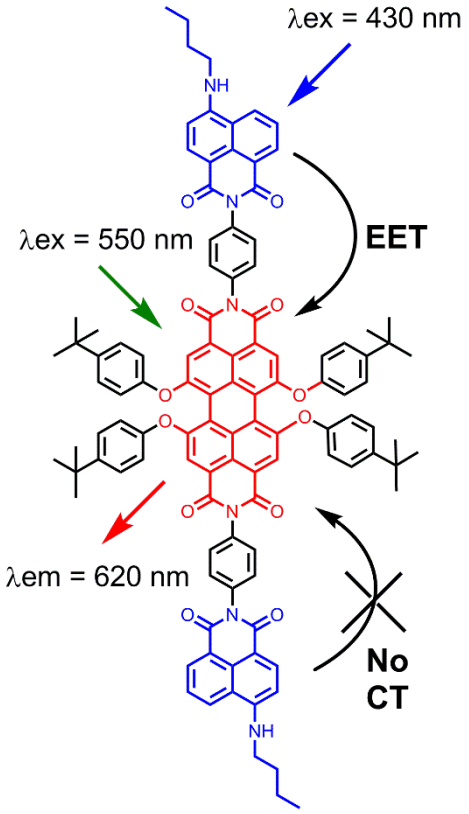

1. **Donor and acceptor are decoupled in the ground state**
   Absorption spectrum of Im-D2A4 equals those of A4 and two D2
   Computational calculations

2. **EET efficiency = 100%**
   Donor´s emission completely qeuenched (upon donor excitation at 430 nm)
   Absorption and fluorescence excitation spectra are identical

3. **Ultrafast excitation energy transfer (EET) with t = 0.6 ps**
   TA measurements at donor excitation (λ_{ex} = 430nm)

4. **Singlet excited state of perylene is formed**
   Perylene´s emission spectrum is observed (upon donor excitation at 430 nm)
   Singlet excited state is observed in TA measurements (upon donor excitation at 430 nm)

5. **Modest quenching of perylene´s excited state**
   Φ_F of Im-D2A4 is 35% lower than that of A4
   Fluorescence life-time is lower than that of A4

6. **Quenching of perylene´s excited state is not by charge transfer (CT)**
   Lower Φ_F of Im-D2A4 is observed regardless of solvent polarity (toluene, $CHCl_3$, benzonitrile)
   Charge-separated species is not observed in TA measurements

Figure S13. Summary of the photophysical properties of Im-D2A4, along with the experimental evidence provided in this report.

4. Energies of Charge Separation:

Rehm-Weller Equation

$$\Delta G^{0}_{CS} = [E_{ox}(D) - E_{red}(A)] - E_{00}(A) - \frac{e^2}{r_{DA}\varepsilon_s} + e^2\left(\frac{1}{2r_D} + \frac{1}{2r_A}\right)\left(\frac{1}{\varepsilon_s} - \frac{1}{\varepsilon_{ref}}\right) \quad \text{(Eq S3)}$$

In the Rehm-Weller equation, E_{ox} *(D)* and E_{red} *(A)* are the oxidation potential of the donor and the reduction potential of the acceptor, respectively, measured in the reference solvent dichloromethane, and E_{00} *(A)* is the spectroscopic excited state energy of the acceptor. In this equation r_D and r_A are the ionic radii of the donor and acceptor radical ions, r_{DA} is the donor-acceptor distance, while ε_{ref} and ε_s are the dielectric constants of the reference solvent dichloromethane and the chosen solvent, respectively. Using the Rehm-Weller equation is a rather crude approximation, as it assumes the formation of spherical ions and approaches the charge separation energy by point charges at the center to center distance between the chromophores r_{DA}. Because the ionic radii r_D and r_A and the interchromophoric distance r_{DA} are of similar magnitude, it is difficult to determine what the effective charge separation distance is. The ionic radius of the perylene acceptor r_A= 7.4 Å, was taken from the literature,[12] and for the ionic radius of the naphthalene acceptor r_D, a value of 3.5 Å was estimated. For the charge separation distance of **Im-D2A2** and **Im-D2A4**, r_{DA} , 13 Å was taken, a value intermediate between the center to center distance of 14.3 Å and the minimum distance of 10.9 Å. Margins of error were calculated using the uncertainties in r_A, r_D, and r_{DA}. It is obvious that in the apolar solvent toluene, the margins of error in the calculated charge separation energies are significant, whereas the values calculated for benzonitrile are more accurate. Excitation energies for the chromophores were corrected for the different solvents, by taking the solvent shift of the spectra into account. Finally, the charge separation energies were calculated using Eq S3 by using following input data: r_D= 3.5 Å r_A= 7.4 Å r_{DA}= 10 Å for **DxAy**[13] and 13 Å for **Im-DxAy**, ε_{Tol}= 2.38, ε_{CHL}= 4.81, ε_{DCM}= 8.93, ε_{Bzn}= 25.9.

Table S2. Energies of charge separation from the excited acceptor, calculated using Eq S3.

Comp	In Tol (eV) ±0.18	In Chl (eV) ±0.1	In Bzn (eV) ±0.03
Im-D2A2	0.23	-0.16	-0.45
Im-D2A4	0.43	0.02	-0.31
D2A2	0.09	-0.23	-0.46
D2A3	0.06	-0.26	-0.51

Table S3. Energies of charge separation from the excited acceptor and the excited donor in toluene:

Comp	Naphthalene imide		Perylene					
	$E_{1/2\ ox}$[a]	E_{S1}[b] (eV)	$E_{1/2\ red}$[a]	E_{S1}[c] (eV)	$e^2/r_{DA}\varepsilon_s$ *±0.1* (eV)	B[g] *±0.06* (eV)	ΔG^0_{CS}[c] *±0.18* (eV)	ΔG^0_{CS}[d] *±0.18* (eV)
D2A2	+0.80	2.6	−1.33	2.37	0.61	0.94	0.09	-0.14
D2A3	+0.80	2.6	−1.09	2.15	0.61	0.94	0.06	-0.39
Im-D2A2	+0.80	2.6	−1.33	2.37	0.47	0.94	0.23	0
Im-D2A4	+0.80	2.6	-1.17	2.01	0.47	0.94	0.43	-0.16

[a]Scan rate 0.10 V/s in dichloromethane. [b]Energy of the first singlet excited-state from absorption and emission measurements. [c]Driving force for charge separation with respect to perylene singlet excited-state, according to Eq S3. [d]Driving force for charge separation with respect to naphthalene imide singlet excited-state, according to Eq S3. [e]Calculated oxidation potential. No oxidation signal was detected in the measured potential window. [f]Value taken from compound **A1**. [g]$B = e^2(1/2r_D+1/2r_A)(\ 1/\varepsilon_s+1/\varepsilon_{ref})$

Table S4. Energies of charge separation from the excited acceptor and the excited donor in chloroform:

Comp	Naphthalene imide		Perylene					
	$E_{1/2\ ox}$[a]	E_{S1}[b] (eV)	$E_{1/2\ red}$[a]	E_{S1}[c] (eV)	$e^2/r_{DA}\varepsilon_s$ *±0.06* (eV)	B[g] *±0.04* (eV)	ΔG^0_{CS}[c] *±0.1* (eV)	ΔG^0_{CS}[d] *±0.1* (eV)
D2A2	+0.80	2.56	−1.33	2.35	0.30	0.29	-0.23	-0.43
D2A3	+0.80	2.56	−1.09	2.15	0.30	0.29	-0.26	-0.69
Im-D2A2	+0.80	2.56	−1.33	2.35	0.23	0.29	-0.16	-0.37
Im-D2A4	+0.80	2.56	-1.17	2.01	0.23	0.29	0.02	-0.53

[a]Scan rate 0.10 V/s in dichloromethane. [b]Energy of the first singlet excited-state from absorption and emission measurements. [c]Driving force for charge separation with respect to perylene singlet excited-state, according to Eq S3. [d]Driving force for charge separation with respect to naphthalene imide singlet excited-state, according to Eq S3. [e]Calculated oxidation potential. No oxidation signal was detected in the measured potential window. [f]Value taken from compound **A1**. [g]$B = e^2(1/2r_D+1/2r_A)(1/\varepsilon_s+1/\varepsilon_{ref})$

Table S5. Energies of charge separation from the excited acceptor and the excited donor in benzonitrile:

Comp	Naphthalene imide		Perylene					
	$E_{1/2\ ox}$[a]	E_{S1}[b] (eV)	$E_{1/2\ red}$[a]	E_{S1}[c] (eV)	$e^2/r_{DA}\varepsilon_s$ *±0.01* (eV)	B[g] *±0.03* (eV)	ΔG^0_{CS}[c] *±0.05* (eV)	ΔG^0_{CS}[d] *±0.05* (eV)
D2A2	+0.80	2.49	−1.33	2.31	0.06	-0.22	-0.46	-0.64
D2A3	+0.80	2.49	−1.09	2.11	0.06	-0.22	-0.51	-0.88
Im-D2A2	+0.80	2.49	−1.33	2.31	0.04	-0.22	-0.45	-0.63
Im-D2A4	+0.80	2.49	-1.17	2.01	0.04	-0.22	-0.31	-0.79

[a]Scan rate 0.10 V/s in DCM. [b]Energy of the first singlet excited-state from absorption and emission measurements. [c]Driving force for charge separation with respect to perylene singlet excited-state, according to Eq S3. [d]Driving force for charge separation with respect to naphalene imide singlet excited-state, according to Eq S3. [e]Calculated oxidation potential. No oxidation signal was detected in the measured potential window. [f]Value taken from compound **A1**. [g]$B = e^2(1/2r_D+1/2r_A)(1/\varepsilon_s+1/\varepsilon_{ref})$

5. Excited state calculations:

The calculations for both **Im-D2A4** and **D2A3** molecules indicate that the main excited states reached by photoexcitation are localized excited states, either on the donor or the acceptor. For **Im-D2A4** the different excited states are fully decoupled, while for **D2A3** there is some extension of the molecular orbitals over the linker between the donor and acceptor (see HOMO-2). This can be understood since the linker in **D2A3** is directly coupled to the conjugated core of the acceptor.

Table S6. Excitation energies, oscillator strengths and main contributions to the excited state for truncated molecule **Im-D2A4**.

E_{exc}(eV)	λ (nm)	*f*	Main contributions
2.19	566	0.96	0.68 (H→L)
2.67	464	0.09	0.61 (H-4 → L)
3.38	367	1.27	0.47 (H-6 → L+1) + 0.47 (H-5 → L+2)

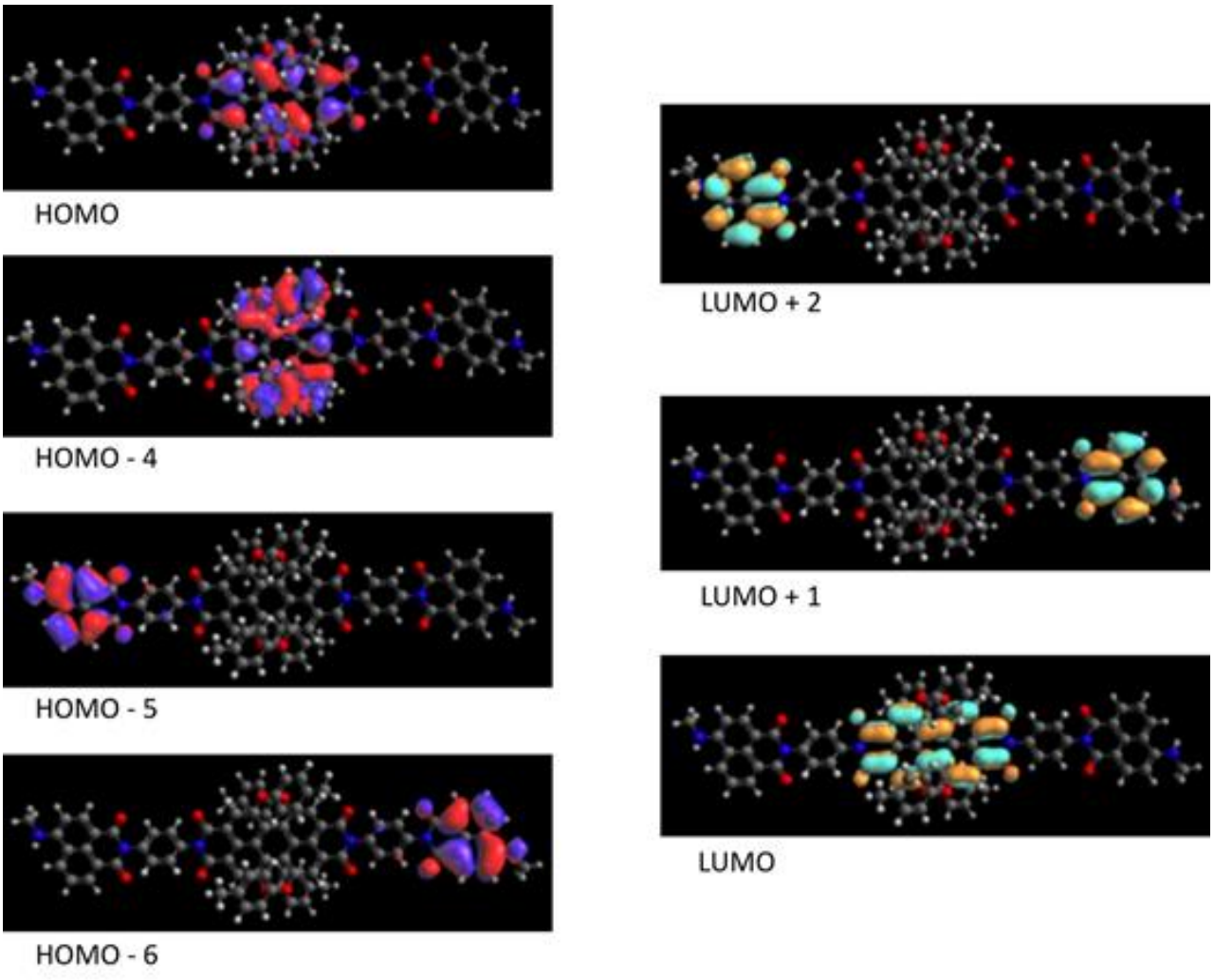

Figure S14. Relevant molecular orbitals for truncated **Im-D2A4**.

Table S7. Excitation energies, oscillator strengths and main contributions to the excited state for molecule truncated **D2A3**.

E_{exc}(eV)	λ (nm)	*f*	Main contributions
2.39	519	1.23	0.68 (H→L)
3.23	384	0.27	0.38 (H-2 → L)
3.37	368	1.19	-0.38 (H-5 → L+1) + 0.31 (H-4→ L+1) + 0.41 (H-3→L+2)

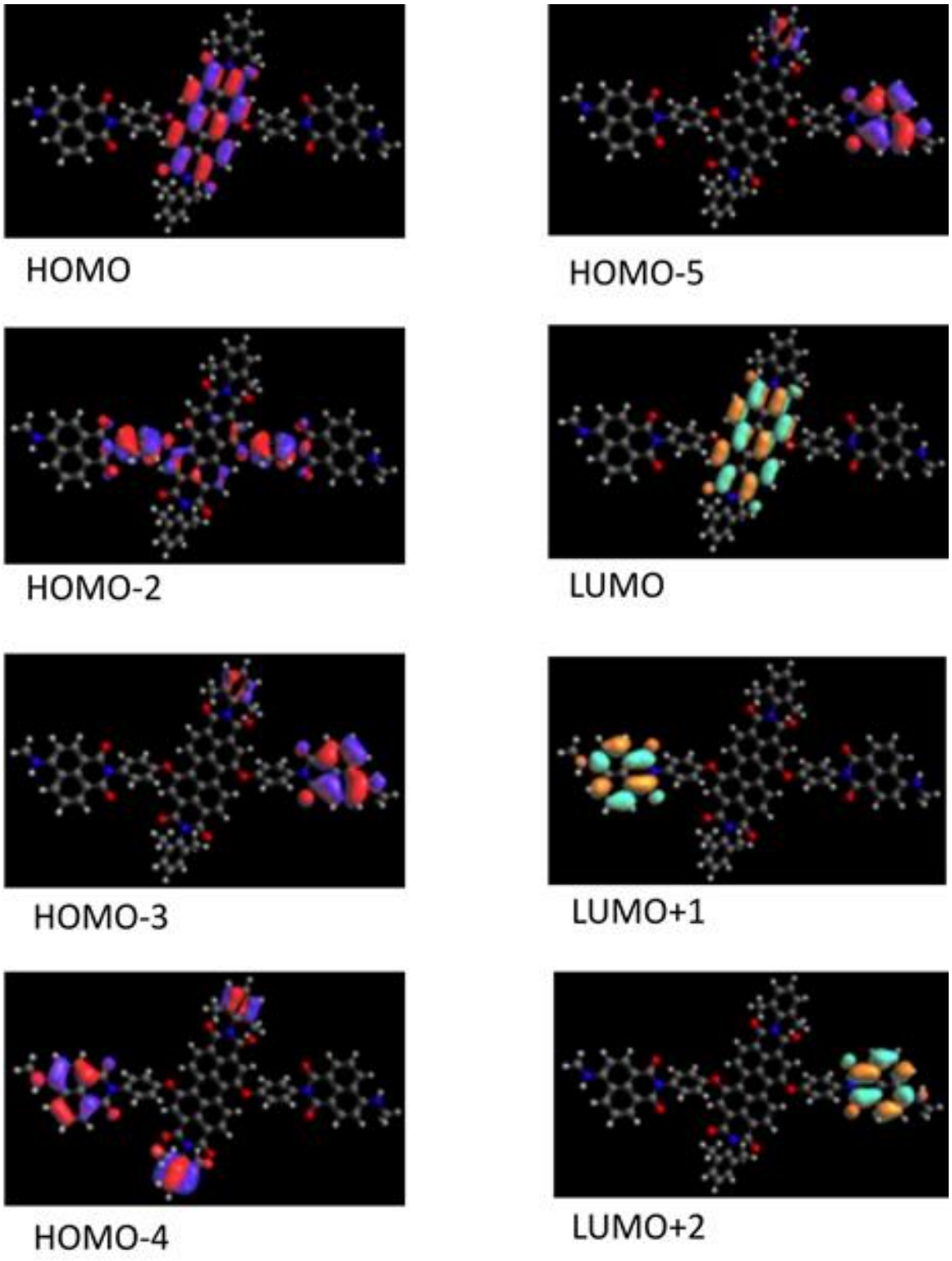

Figure S15. Relevant molecular orbitals for truncated **D2A3**.

6. ^{1}H NMR and HR-mass Spectra:

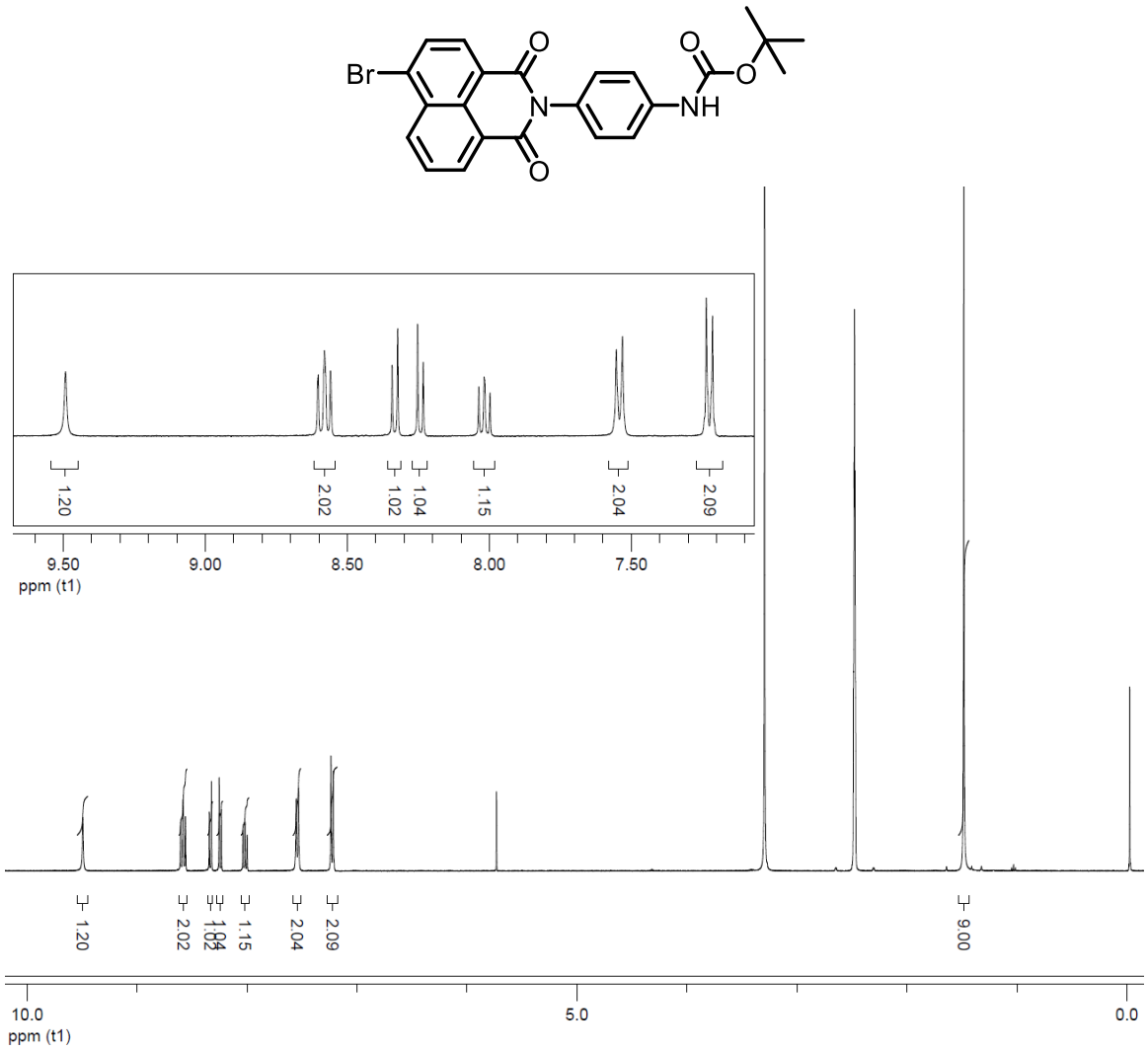

Figure S5.1. ^{1}H NMR spectrum of *N*-[(4′ -Boc-amino)phenyl]-4-bromonaphthalene-1,8-dicarboxy Monoimide (**7**) in DMSO-d6.

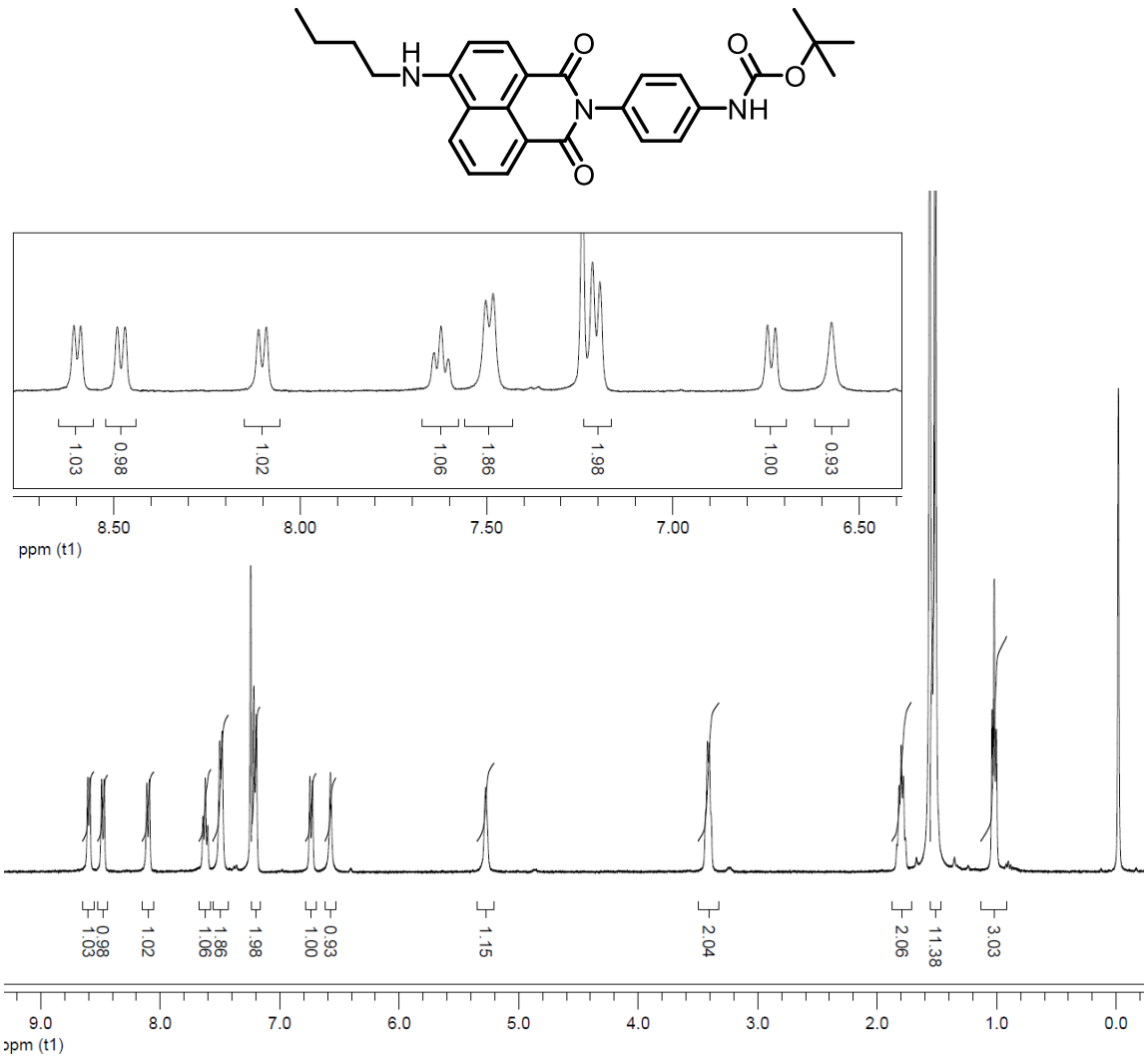

Figure S5.2. ^{1}H NMR spectrum of *N*-[(4′-Boc-amino)phenyl]-4-(*n*-butylamino)naphthalene-1,8-dicarboxy Monoimide (**8**) in $CDCl_3$.

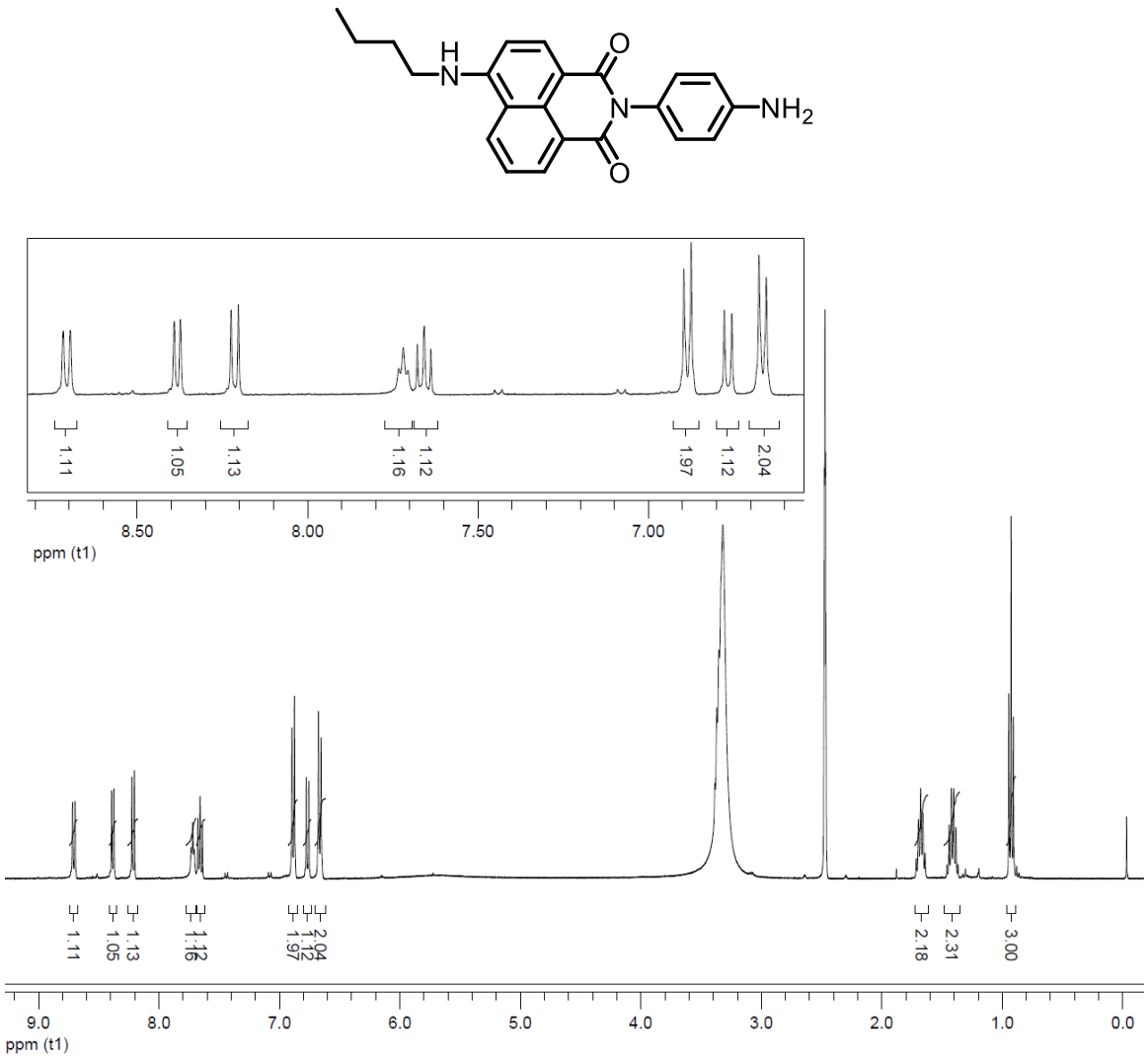

Figure S5.3. ^{1}H NMR spectrum of *N*-(4′-aminophenyl)-4-(*n*-butylamino)naphthalene-1,8-dicarboxy Monoimide (**2**) in DMSO-d6.

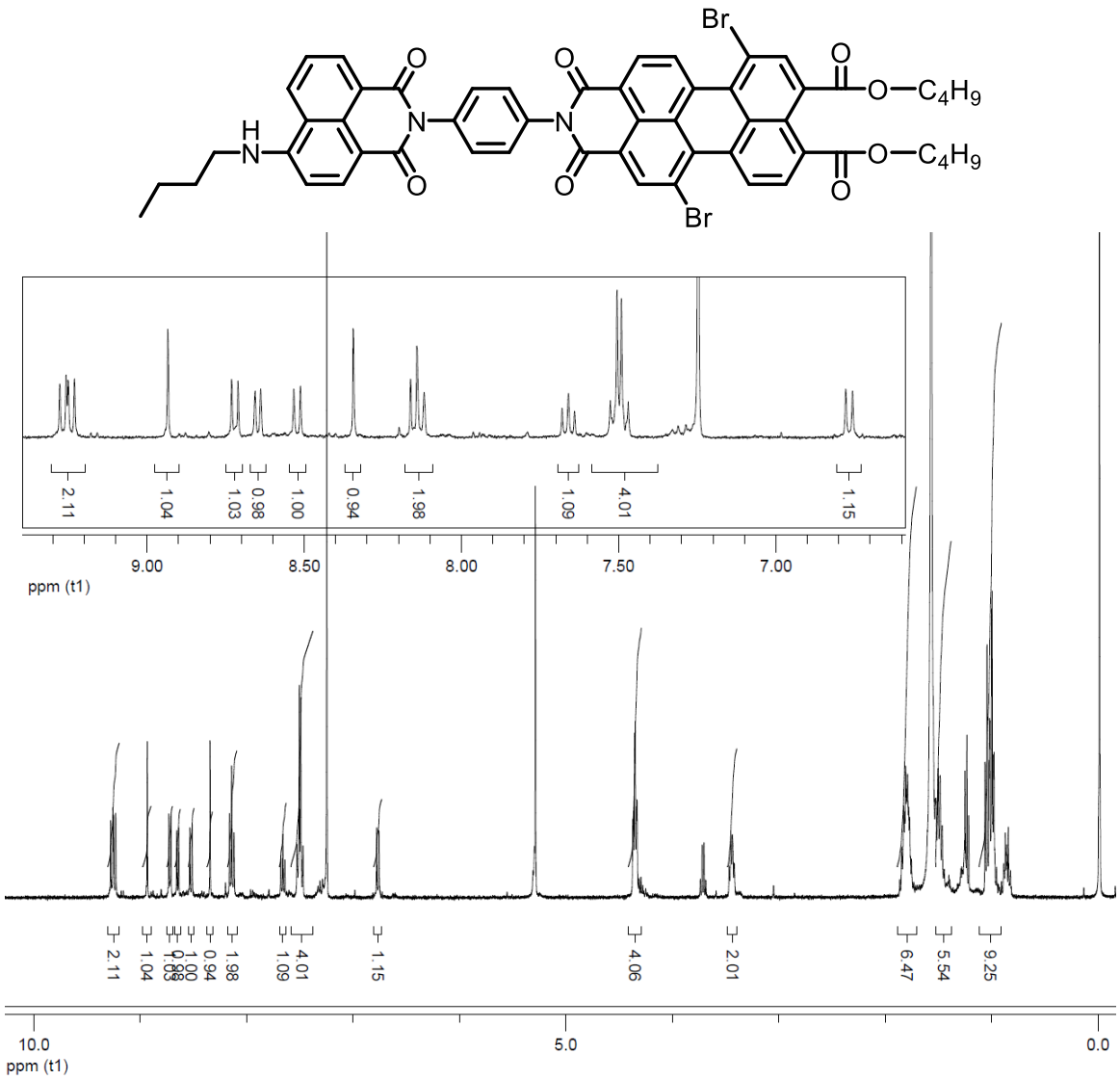

Figure S5.4. ^{1}H NMR spectrum of compound **3** in $CDCl_3$.

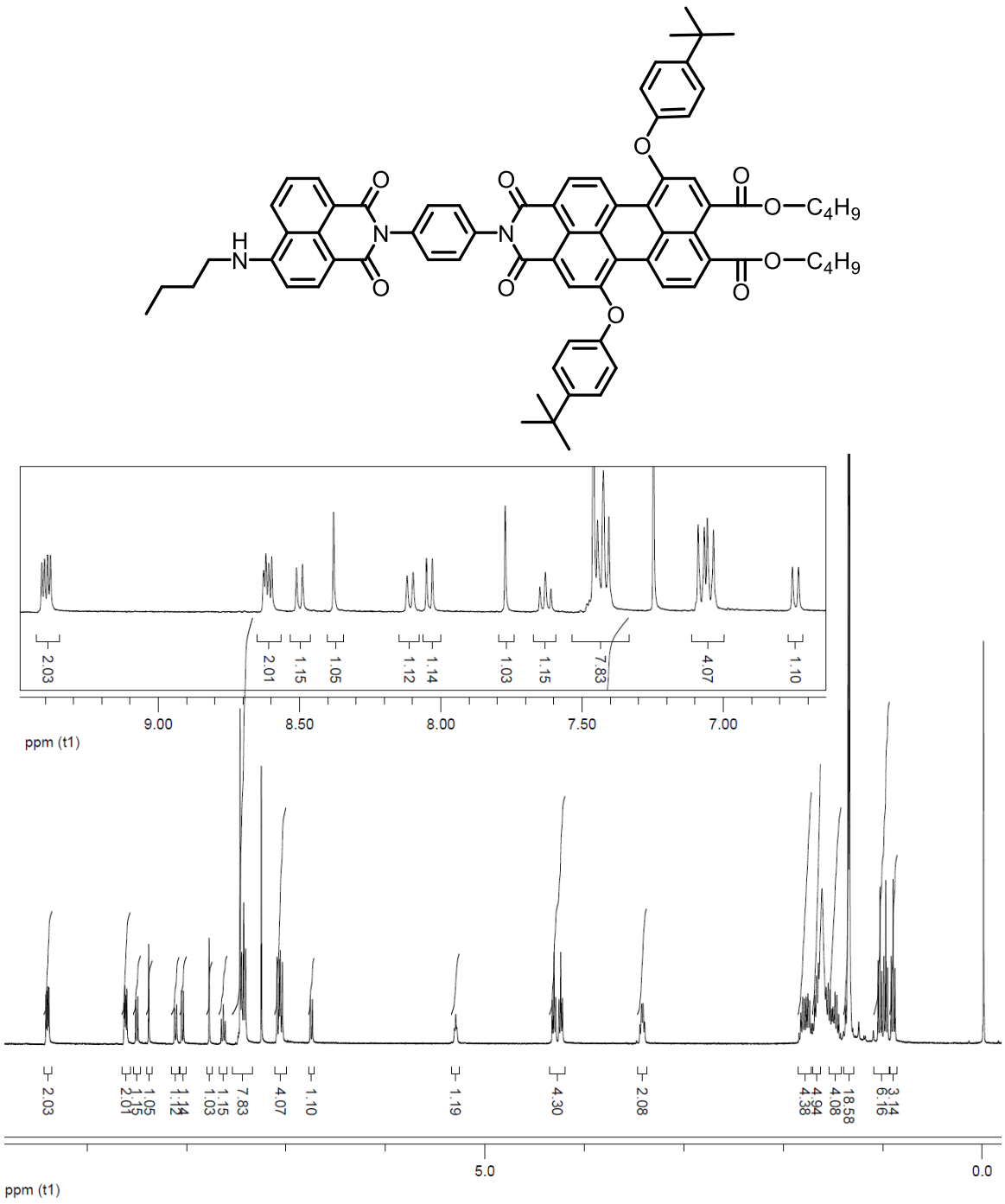

Figure S5.5. ^{1}H NMR spectrum of **Im-D2A2** in $CDCl_3$.

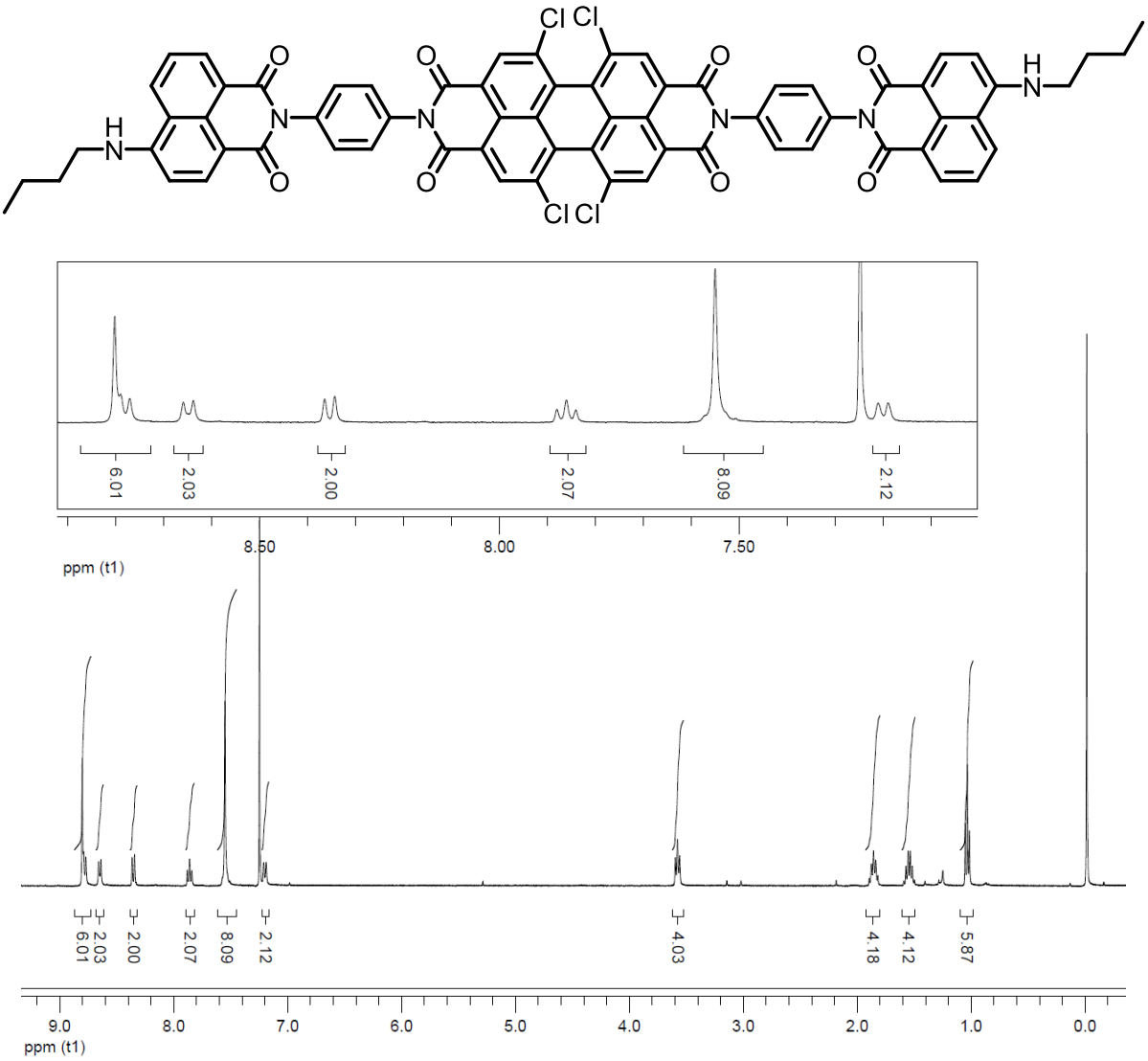

Figure S5.6. ^{1}H NMR spectrum of compound **5** in $CDCl_3$.

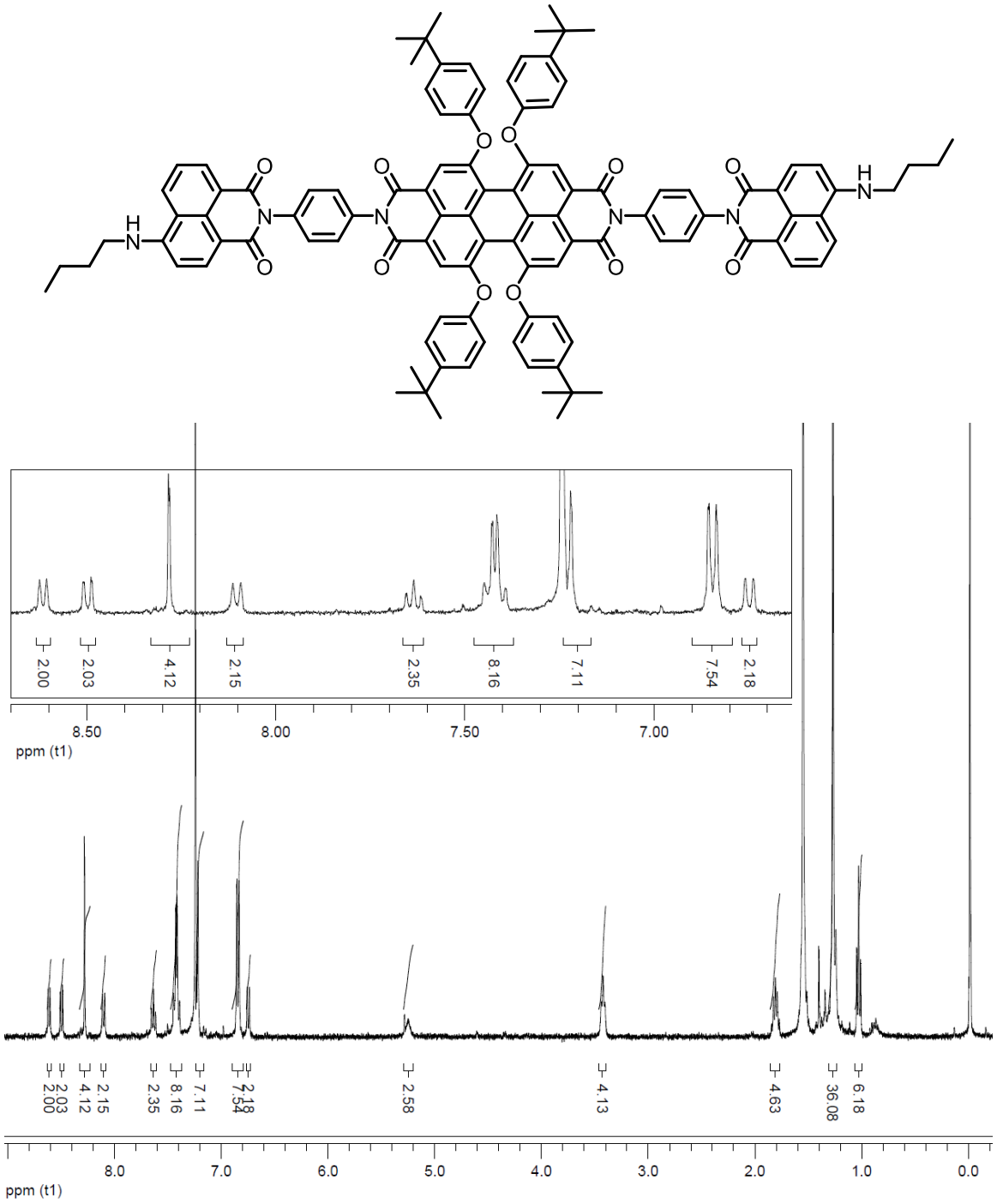

Figure S5.7. ^{1}H NMR spectrum of compound **Im-D2A4** in $CDCl_3$.

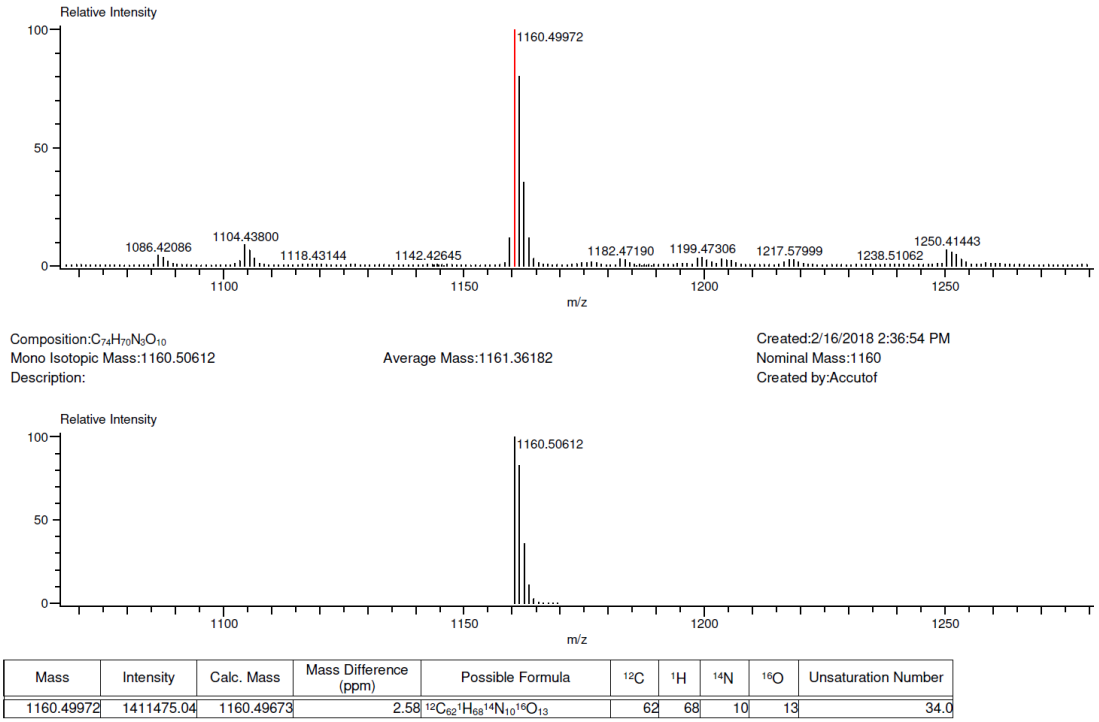

Mass	Intensity	Calc. Mass	Mass Difference (ppm)	Possible Formula	^{12}C	^{1}H	^{14}N	^{16}O	Unsaturation Number
1160.49972	1411475.04	1160.49673	2.58	$^{12}C_{62}{}^{1}H_{68}{}^{14}N_{10}{}^{16}O_{13}$	62	68	10	13	34.0

Figure S5.8. HR mass spectrum of **Im-D2A2**.

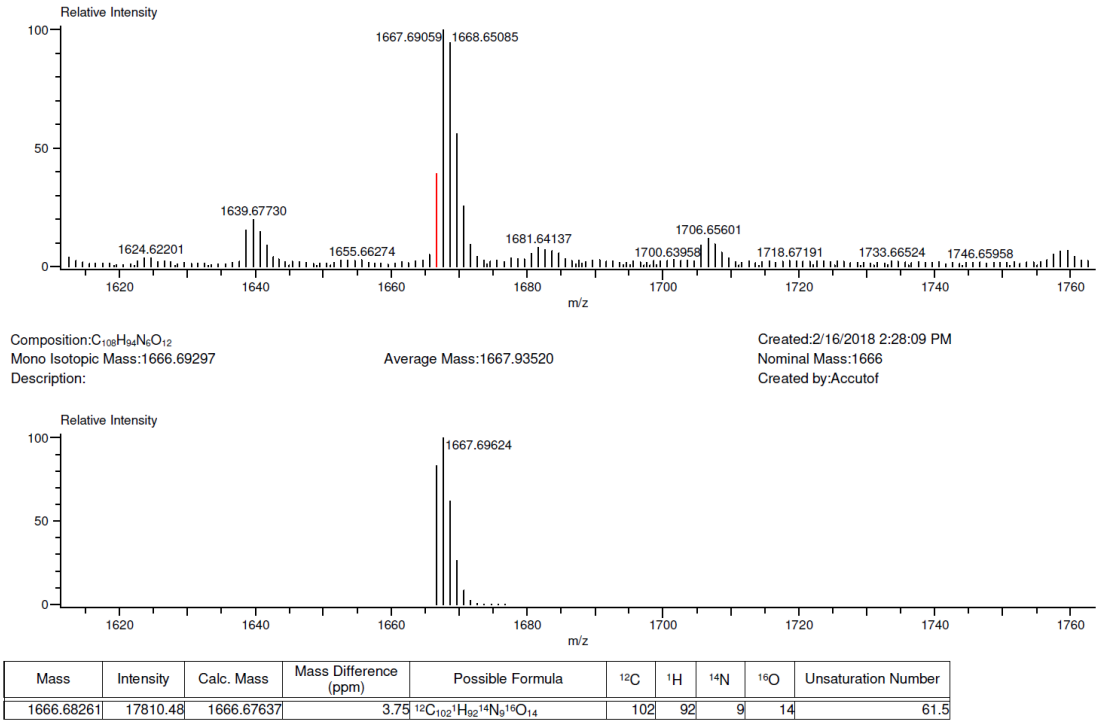

Mass	Intensity	Calc. Mass	Mass Difference (ppm)	Possible Formula	^{12}C	^{1}H	^{14}N	^{16}O	Unsaturation Number
1666.68261	17810.48	1666.67637	3.75	$^{12}C_{102}{}^{1}H_{92}{}^{14}N_{8}{}^{16}O_{14}$	102	92	8	14	61.5

Figure S5.9. HR mass spectrum of compound **Im-D2A4**.

7. References

1. S. Sengupta, R. K. Dubey, R. W. M. Hoek, S. P. P. van Eeden, D. D. Gunbaş, F. C. Grozema, E. J. R. Sudhölter and W. F. Jager, *The Journal of Organic Chemistry*, 2014, **79**, 6655-6662.
2. R. K. Dubey, N. Westerveld, F. C. Grozema, E. J. R. Sudhölter and W. F. Jager, *Organic Letters*, 2015, **17**, 1882-1885.
3. R. K. Dubey, N. Westerveld, E. J. R. Sudholter, F. C. Grozema and W. F. Jager, *Organic Chemistry Frontiers*, 2016, **3**, 1481-1492.
4. G. A. Crosby and J. N. Demas, *The Journal of Physical Chemistry*, 1971, **75**, 991-1024.
5. H. Langhals, J. Karolin and L. B-A. Johansson, *Journal of the Chemical Society, Faraday Transactions*, 1998, **94**, 2919-2922.
6. J. J. Snellenburg, S. Laptenok, R. Seger, K. M. Mullen and I. H. M. van Stokkum, *2012*, 2012, **49**, 22.
7. I. H. M. van Stokkum, D. S. Larsen and R. van Grondelle, *Biochimica et Biophysica Acta (BBA) - Bioenergetics*, 2004, **1657**, 82-104.
8. G. te Velde, F. M. Bickelhaupt, E. J. Baerends, C. Fonseca Guerra, S. J. A. van Gisbergen, J. G. Snijders and T. Ziegler, *Journal of Computational Chemistry*, 2001, **22**, 931-967.
9. Gaussian 09, M. J. Frisch, G. W. Trucks, H. B. Schlegel, G. E. Scuseria, M. A. Robb, J. R. Cheeseman, G. Scalmani, V. Barone, G. A. Petersson, H. Nakatsuji, X. Li, M. Caricato, A. Marenich, J. Bloino, B. G. Janesko, R. Gomperts, B. Mennucci, H. P. Hratchian, J. V. Ortiz, A. F. Izmaylov, J. L. Sonnenberg, D. Williams-Young, F. Ding, F. Lipparini, F. Egidi, J. Goings, B. Peng, A. Petrone, T. Henderson, D. Ranasinghe, V. G. Zakrzewski, J. Gao, N. Rega, G. Zheng, W. Liang, M. Hada, M. Ehara, K. Toyota, R. Fukuda, J. Hasegawa, M. Ishida, T. Nakajima, Y. Honda, O. Kitao, H. Nakai, T. Vreven, K. Throssell, J. A. Montgomery, Jr., J. E. Peralta, F. Ogliaro, M. Bearpark, J. J. Heyd, E. Brothers, K. N. Kudin, V. N. Staroverov, T. Keith, R. Kobayashi, J. Normand, K. Raghavachari, A. Rendell, J. C. Burant, S. S. Iyengar, J. Tomasi, M. Cossi, J. M. Millam, M. Klene, C. Adamo, R. Cammi, J. W. Ochterski, R. L. Martin, K. Morokuma, O. Farkas, J. B. Foresman, and D. J. Fox, Gaussian, Inc., Wallingford CT, 2016.
10. M. D. Hanwell, D. E. Curtis, D. C. Lonie, T. Vandermeersch, E. Zurek and G. R. Hutchison, *Journal of Cheminformatics*, 2012, **4**, 17.
11. J. R. Lakowicz, *Principles of Fluorescence Spectroscopy, Chapter 13*, Kluwer Academic and Plenum Publishers: New York, Second edn., 1999.

12. R. H. Goldsmith, L. E. Sinks, R. F. Kelley, L. J. Betzen, W. Liu, E. A. Weiss, M. A. Ratner and M. R. Wasielewski, *Proceedings of the National Academy of Sciences of the United States of America*, 2005, **102**, 3540-3545.
13. D. Inan, R. K. Dubey, W. F. Jager and F. C. Grozema, *The Journal of Physical Chemistry C*, 2019, **123**, 36-47.